RAYLEIGH WAVE DISPERSION CURVE INVERSION COMBINING WITH GA AND DSL

YUHANG LEI, HONGYAN SHEN, SHENGJIE XIE and YIDONG LI

School of Earth Sciences and Engineering, Xi'an Shiyou University, Xi'an Shaan'xi 710065, P.R. China. Shenhongyan@xsyu.edu.cn

(Received July 13, 2017; revised version accepted January 12, 2018)

ABSTRACT

Lei, Y.H., Shen, H.Y., Xie, S.J. and Li, Y.D., 2018. Rayleigh wave dispersion curve inversion combining with GA and DSL. *Journal of Seismic Exploration*, 27: 151-165.

Rayleigh wave dispersion curve inversion is a multi-parameter highly non-linear iterative optimization process. The conventional single linear or non-linear inversion method has some limitations for the complex seismic geologic conditions, which can lead to more prominent multi-solution problem. But the defects both of the methods can be supplemented by the advantages of each other. In order to further improve the inversion accuracy, we proposed a joint inversion method via complementing and nesting the linear (damping least squares) and non-linear (genetic algorithm) methods. Firstly, the genetic algorithm (GA) is utilized based on the loose constraints of prior geological information to lock in the target near the global optimal solution. Then, use the damping least squares (DLS) method to achieve higher precision of Rayleigh wave dispersion curve inversion. The effectiveness of the method has been verified by a typical layered model. And we use the method to further process actual seismic data. Results show that the method not only absorbs the advantages of GA with global optimization and strong adaptability, but also inherits the advantages of DLS with fast convergence and stable inversion. And better results are achieved in suppressing multi-solution, getting rid of the initial model highly dependent, and improving inversion accuracy.

KEY WORDS: Rayleigh wave, dispersion curves, genetic algorithm (GA), damping least squares (DLS), joint inversion.

INTRODUCTION

Shear wave velocity is an essential parameter to characterize geotechnical properties in geophysical survey, and also is an important basis for stratigraphic structure division. Surface wave dispersion curve inversion is an efficient means to obtain the shear-wave velocity (Malagnini et al., 1995; Park et al., 1999; Xia et al., 2015; Moro et al., 2003; Yilmaz et al.,

0963-0651/18/$5.00

2005). It has been widely used in geotechnical investigation (Xia et al., 2004; Sussmann et al., 2015; Chang et al., 2016), geological disaster investigation (Caldwell et al., 2009; Júnior et al., 2012), coal field and oil-gas field exploration (Laake et al., 2008; Strobbia et al., 2010a,b, 2011) and other fields. All these also contributed to the rapid development of Rayleigh wave dispersion curve inversion techniques. For the surface wave dispersion curve inversion, from the beginning to use the inflection point method (Nazarian et al., 1983), asymptotic line method, approximate calculation method and simplified stripping method (Cui et al., 1994) to now have been basically formed linear and non-linear two inversion theory system. Linear inversion method is more perfect that has been adopted widely because of the fast convergence, high precision, good stability and other advantages (Xia et al., 1999, 2002a,b, 2012; Chen et al., 2006). However, Rayleigh wave dispersion curve inversion is a height non-linear iterative optimization process with multiple parameters. Local optimization makes it depend seriously on the initial model (Moro et al., 2007a). Some processing means have been adopted, such as equivalent replacing the weak sensitivity parameters using others based on the sensitivity analysis (Xia et al., 1999), and divided stratigraphic into several equal thickness layers (Luo et al., 2008), which weaken the initial model requirements and have achieved some better effects on repressive multi-solution of inversion. It is also very effective to improve the inversion accuracy and enhance the stability of the results when simultaneously inverting the fundamental and higher mode data (Xia et al., 2003; Luo et al., 2008). Even so, the linear method above is easily falls into local extremum during the inversion process due to the superposition of different components of the seismic wave field, the influence of the external disturbance factors and improper initial model. It may lead to a greater difference between the inversion result and the actual geological situation that will inevitably affect the accuracy of geological interpretation (Luo et al., 2008; Guo et al., 2015). More seriously, if the prior geological information is not sufficient, the linear inversion will fail. In contrast, genetic algorithms (Moro et al., 2007a, b), simulated annealing (Beaty et al., 2002), artificial neural networks (Meier et al., 1993) and other non-linear inversion methods are not strict for initial model requirement, which more suitable for complex geological issues (such as fractured zone, low velocity interlayer, thin layer, blind layer, etc.). The inversion results based on global optimization search are more likely to match the actual geophysical model in theory (Yamanaka et al., 1996; Lu et al., 2014). However, in order to obtain accurate inversion results, such as for the GA inversion method, we must rely on a large population selection and higher training times, which will lead to slower convergence, a huge amount of calculation and other issues (Moro et al., 2003, 2007a,b). The global optimization direction of the non-linear inversion is unpredictable because of the more inversion parameters. The resulting "premature" and effective genes loss are also greatly increased by randomness and uncertainty (Liu et al., 2017).

For the above problems, we attempt to invert the Rayleigh wave dispersion curve combining with linear and non-linear inversion (mainly GA

and DLS). It is designed to suppress the inversion multi-solution, reduce the dependence of the initial model, and improve the inversion efficiency and accuracy.

METHODOLOGY

Model forward

The actual formation generally has the characteristics of stratification and velocity gradient. So, it can be equivalent to a multi-layer elastic solid medium model with a horizontal free interface. In the paper, forward modeling is carried out based on this structure, and a dispersion curve is obtained by fast Knopoff method (Knopoff, 1964).

Loose constraints for inversion parameters

The non-linear implicit Rayleigh wave dispersion equation about stratigraphic parameters can be expressed as (Xia et al., 1999),

$$v_{Ri}=G(f_i,\boldsymbol{v}_S,\boldsymbol{v}_P,\boldsymbol{h},\boldsymbol{\rho}) \quad (i = 1,2,\ldots,m) \quad , \tag{1}$$

where, f_i is the i-th frequency, v_{Ri} is the phase velocity at frequency f_i, $\boldsymbol{v}_S = (v_{S1}, v_{S2}, \ldots, v_{Sn})^T$ is the shear wave velocity vector, $\boldsymbol{v}_P = (v_{P1}, v_{P2}, \ldots, v_{Pn})^T$ is the compressional wave velocity vector, $\boldsymbol{h} = (h_1,h_2,\ldots,h_{n-1})^T$ is the thickness vector, $\boldsymbol{\rho} = (\rho_1, \rho_2,\ldots, \rho_n)^T$ is the density vector, m is the number of actual measured phase velocity, and n is the number of layers. Parameter vectors above can be obtained as follows:

The research shows that the influence of $\boldsymbol{v}_P$ and $\boldsymbol{\rho}$ on the dispersion curve is relatively small (Xia et al., 1999). Therefore, eq. (1) can be expressed as an equation which only contains $\boldsymbol{v}_S$ and $\boldsymbol{h}$. They can be calculated by Rayleigh wave penetration formula eq. (2) (Shen et al., 2016) and the relationship between Rayleigh wave velocity phase v_R and shear wave velocity v_S eq. (3) (Chen et al., 2006).

$$H_i = \beta\lambda_{Ri} \quad (i = 1,2,\ldots,m) \quad \beta \in (0.55,0.87) \quad , \tag{2}$$

where, H is penetration depth, β is penetrating factor associated with Poisson's ratio, λ_{Ri} is Rayleigh wave wavelength.

$$v_{Ri} = \frac{0.862+1.14\sigma}{1+\sigma} v_{Si} \quad (i=1, 2,\ldots, m) \quad \sigma\in(0,0.5) \quad , \tag{3}$$

where, σ is Poisson's ratio.

The feasible solution ranges of the formation parameters determined by eq. (2) and eq. (3) cannot be used accurately by DLS inversion, but it provides a global optimal retrieval space for GA inversion.

GA inversion

GA is an adaptive global optimization random search algorithm which is formed by simulating the genetic and evolutionary processes of biological organisms in natural environment. It is achieved through operations, selection, crossover and mutation (Yamanaka et al., 1996). The processing flowchart is shown in Fig. 1, and the specific operation is as follows:

(1) Use binary coding to map the stratigraphic parameters into between 0 and 2^l. The resolution of the inversion parameters is determined by the coded bits number l ($l \in Z$).

(2) Use random function to randomly generate individuals P_j ($\boldsymbol{v}_S$, $\boldsymbol{v}_P$, $\boldsymbol{h}$, $\boldsymbol{\rho}$), and then form a initial population. The objective function values of each individual are calculated by eq. (4) (Moro et al., 2007a).

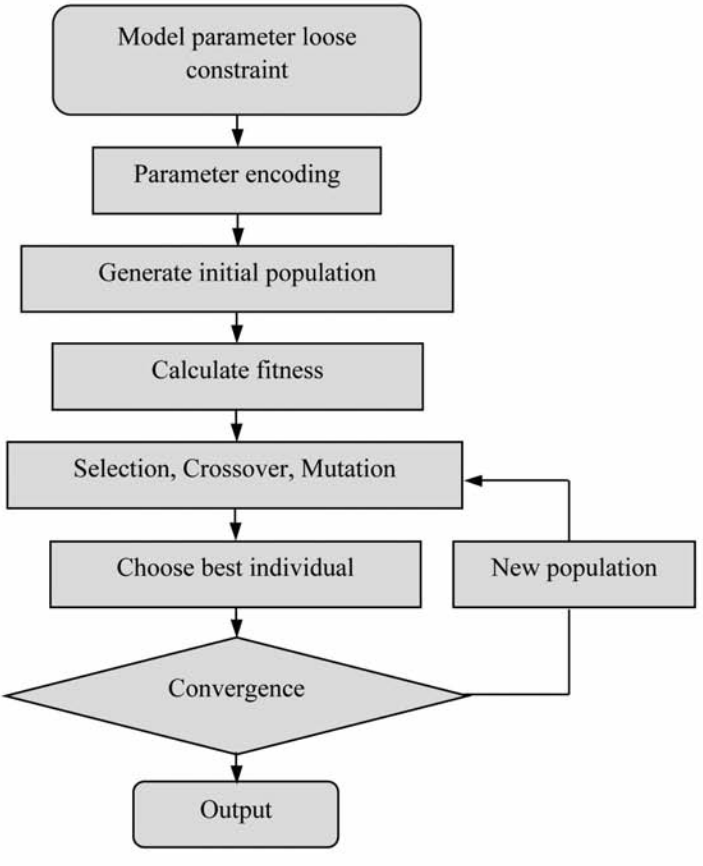

Fig. 1. Processing flowchart of GA inversion.

$$\Phi(P_j) = \sqrt{\frac{\sum_{i=1}^{m} (v_{Ri}^{c}(P_j) - v_{Ri}^{o})^2}{m}} \quad , \qquad (4)$$

where P_j is the j th individual, $v_{Ri}^{c}(P_j)$ [illegible] reference, storage and computation consumption.

0963-0651/18/$5.00

by the model individual P_j, v_{Ri}^{o} is the measured phase velocity, e number of measured phase velocities.

convert the calculated objective function minimum to the search ction maxima according to eq. (5),

$$f(P_j) = \begin{cases} C_{\max} - \Phi(P_j) & \Phi(P_j) < C_{\max} \\ 0 & \text{others} \end{cases} \quad , \qquad (5)$$

P_j) is the fitness of the individual P_j. C_{max} is a larger integer, and lly takes 10~20 times the maximum value of $\Phi(P_j)$ in the in our study (Liu et al., 2017).

the classic roulette way to select the male parent to forming a new . The aim is to retain fine individuals, and eliminate poor s. All individuals in the new population are randomly matched and a certain probability (taking 0.6 in this paper) (Yamanaka et al., g. 2). The crossover at a lower level of the parameter coding is to search at the around of better individual to achieve population on. It is also important to randomly select a coded bit for mutation to maintain the diversity of the population gene. In order to e loss of effective genes, we find the highest fitness individual P_j it in the next generation of new population, and continue the ration in practice.

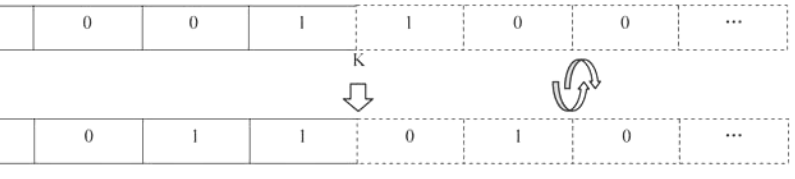

ssover operation diagram of GA inversion. *Px* and *Py* are two individuals lected in the population. Since the K value is usually relatively small, the f the encoding parameters after the encoding bit K is equivalent to the operation in the vicinity of the solution.

calculated
and m is t

Then
fitness fu

where, f (
C_{max} usua
populatio

(3) Adopt
populatio
individual
crossed at
1996) (Fi
equivalen
optimizati
operation
prevent th
and save
genetic ite

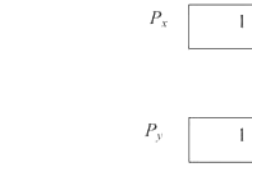

Fig. 2. Cro
randomly s
exchange o
optimizatio

DLS inversion

DLS inversion is a local linear inversion method, which is a combination of the Newton method and the gradient method. The basic idea is to interpolate by the fastest descent method between the corrections $\Delta \boldsymbol{x}$ under the damping factor control so that the objective function $\Phi(\boldsymbol{x})$ advances in the descending direction at a maximum step until convergence (Madsen et al., 2004; Xia et al., 1999). The method consists of two main processes:

1. To establish the inversion target equation.
Dispersion eq. (1) is developed near the initial model $\boldsymbol{x}_0$ by using the Taylor's series expansion. Then subtract measured phase velocity and make it equal to 0, and solve the partial derivation of $\Delta \boldsymbol{x}$ and rewrite it into a matrix form. The inversion equation can be obtained as follows,

$$\boldsymbol{A}^T \boldsymbol{A} \Delta \boldsymbol{x} = \boldsymbol{A}^T [v_{\mathrm{R}}^{\mathrm{c}}(\boldsymbol{x}_0) - v_{\mathrm{R}}^{\mathrm{o}}] \quad , \tag{6}$$

where, $\boldsymbol{A}$ is a differential coefficient matrix that calculated by difference quotient. $v^{\mathrm{o}}_{\mathrm{R}}$, $v^{\mathrm{c}}_{\mathrm{R}}$ represent the measured and calculated phase velocity respectively. The sliding damping factor μ is added to the left of the equation to ensure that the matrix is nonsingular positive definite. And the correction quantity can be solved by

$$\Delta \boldsymbol{x} = (\boldsymbol{A}^T \boldsymbol{A} + \mu \boldsymbol{I})^{-1} \boldsymbol{A}^T [v_{\mathrm{R}}^{\mathrm{c}}(x_0) - v_{\mathrm{R}}^{\mathrm{o}}] \quad , \tag{7}$$

where, $\boldsymbol{I}$ is the unit matrix.

2. Fastest descent method interpolation.
The iterative interpolation is performed base on the calculated $\Delta \boldsymbol{x}$ vector until the objective function satisfies the precision requirement or the parameter correction amount reaches the lower limit. The optimal step length λ is calculated as follows:

$$\lambda = \sum_{k=1}^{N} g_k \Delta x_k \,/\, (\Phi(\boldsymbol{x}_0 + \Delta \boldsymbol{x}) - \Phi(\boldsymbol{x}_0) + 2 \sum_{k=1}^{N} g_k \Delta x_k) \quad , \tag{8}$$

where, $g_k = (\boldsymbol{A}^T \boldsymbol{A} + \mu \boldsymbol{I}) \Delta x_k$ (k = 1,2,…,N), N is the amount of inversion parameters, and Δx_k is the correction value for each parameter.

JOINT GA AND DLS INVERSION

The combination of linear and non-linear nested inversion methods not only absorbs the advantages of GA global optimization and low dependency to the initial model, but also plays a quick convergence and high precision advantages of the DSL method in the local linear space. The Inversion flowchart is shown in Fig. 3. The specific steps are as follows:

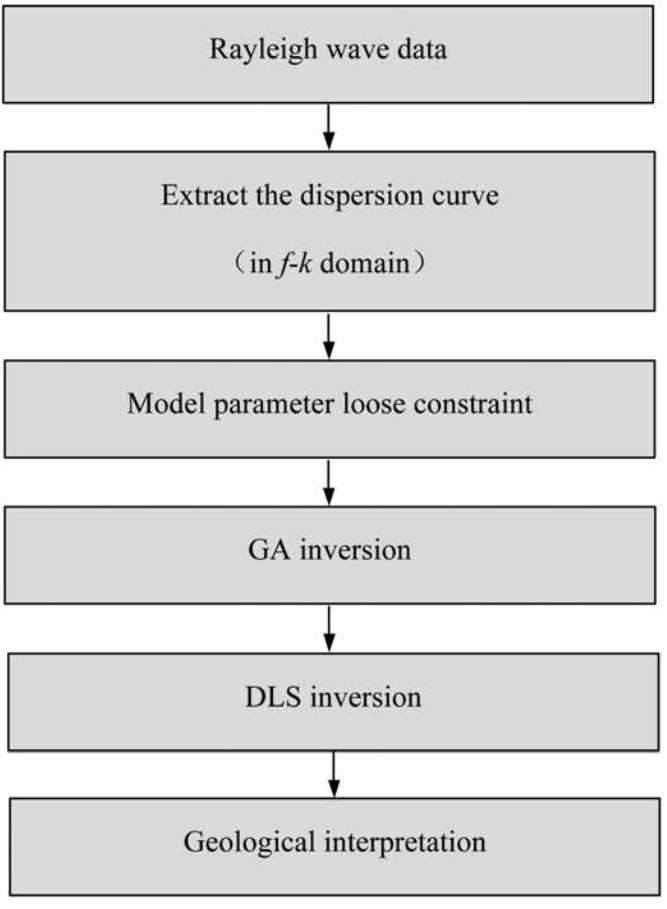

Fig. 3. Processing flowchart of combining with GA and DLS inversion.

1. Extract the Rayleigh wave dispersion curve f-v_R from the dispersion energy spectrum f-v_R (Shen et al., 2016).

2. Based on the characteristic analysis of the measured dispersion curve, determine the upper and lower limits of the model parameters according to the loose constraint described.

3. Use GA inversion to lock the target near the global optimal solution after several iterations.

4. Use the optimization results of GA inversion as the initial model of DLS inversion. And efficient linear interpolates in the local range near the optimal solution until the convergence condition is satisfied and output the inversion results.

MODEL DATA TEST

In order to verify the validity and superiority of jointing GA and DLS to invert the Rayleigh wave dispersion curve, we designed a geological model with horizontal layered homogeneous media to test. The velocities are increasing in the model, and the second layer is a low velocity interlayer. The specific parameters are shown in Table 1.

Table 1. 6-layer geological model parameters.

Layer No.	Δh(m)	v_S(m/s)	v_P(m/s)	ρ(g/cm^3)
1	1.0	280	510	1.47
2	2.0	240	437	1.41
3	3.0	290	528	1.49
4	4.0	320	582	1.52
5	5.0	440	801	1.65
6	∞	620	1128	1.80

Equal thickness DLS inversion

First, we use the conventional equal thickness thin layer method to invert the dispersion of the model. The stratum has been divided into 15 thin layers with thickness of 1 m and a uniform half space layer (16 layers in total). The iterative operation times are 2306, and the final fitting error is 1.30 E^{-6}. The results generally reflect the velocity variation characteristics. But there is a large error in this method compared with the geological model (Fig. 4). In depth analysis is as follows:

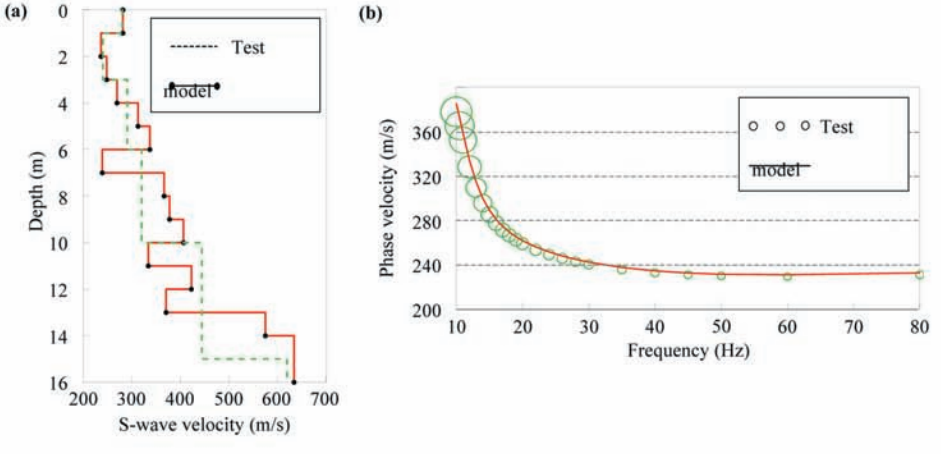

Fig. 4. Equal thickness thin-layer inversion model by DLS. (a) Stratigraphic structure (H-v_S), (b) Dispersion curve (v_{Ph}–f)

1. The first three layers of the inversion results are in good agreement with the geological model. Starting from the low-velocity interlayer, there are some errors and obvious fluctuations in the parameters of each layer. It indicates that the method is not applicable for low-velocity interlayer. There are also few differences of the fitting about both dispersion curves. It shows that the equivalence between the two dispersion curves is the reflection of the inversion multi-solution. In addition, there are four low-velocity layers in the inversion results, but only the first low-velocity layer (from 2 to 3 m, error 4.8%) is the true reflection of the geological model. Other false judgments attributed to the local optimal solution in the local linear optimization process.

2. In principle，the thinner the thickness of each layer in model is divided, the more accurate the inversion results will be. However, the prerequisite should be based on an initial model with a higher precision. Especially in the anomalous stratigraphic model, the determined shear wave velocity by the method (Xia et al., 1999, 2002a,b, 2012; Chen et al., 2006) is too far from the real model, and the inversion result is easily caught in the local optimal solution and even fails.

In conclusion, there are great differences between the DLS inversion results and the test model in the formation structure, the depth of abnormal, and shear wave velocity that reflect the limitations of the linear inversion method.

Combining with GA and DLS inversion

Next, we use the flowchart in Fig. 4 to invert the dispersion curve of the model in Table 1. GA inversion is performed based on the parameter space of initial model determined by the loose constraint (Population number 100, genetic iteration 20 times). Terminate iteration optimization after 127.45 s, and the optimal individual fit residual *obj* is 0.21. The average and best individual fitting residuals of each generation population in the inversion process are shown in Fig. 5 (taking the first 30 individuals of each generation).

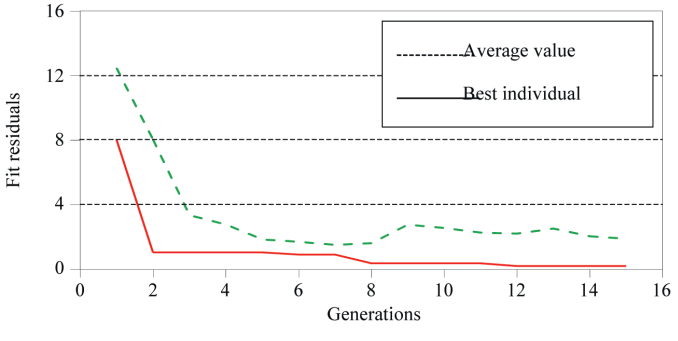

Fig. 5. Fitting residual curve of GA inversion.

In the initial stage of the iteration, all individuals in the population affected by the selective operation are rapidly moving closer to the global optimal, and the fitting residual of the optimal individual is rapidly reduced. After the first step (from the 2nd to the 6th generation), the *obj* again decreased significantly. It suggests that optimize randomly under crossover operation near the global optimal solution. Then, the improvement of the inversion precision is mainly dependent on the mutation operation. The low probability and direction cannot certain of the mutation results in small fluctuations (the 9th generation) in the population fit, but benign mutation (the 11th generation) also promote the optimal individual close to the overall optimal solution. In conclusion, the inversion efficiency of GA becomes very low after 15 times iterative operation. But the target has been locked to near the global solution, which is sufficient to meet the requirements of the initial model of the DLS inversion.

The final inversion results (Fig. 6 and Table 2) are obtained by the DLS based on the model by GA inversion, and the target residual S is only $2.07E^{-11}$. The inversion results show that the joint inversion results with the model are almost completely coincident, and the biggest layer parameter error is only 0.93%.

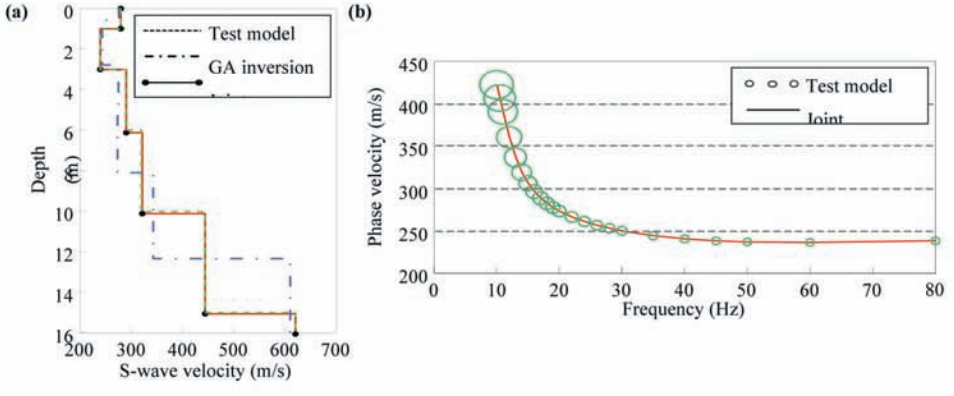

Fig. 6. 6-layer model inversion results combining with GA and DLS inversion. (a) Stratigraphic structure (H-v_S), (b) Dispersion curve (v_{Ph}-f).

Table 2. Joint inversion parameters.

Layer No.	Test Model		Joint Inversion	
	Δh(m)	v_S(m/s)	Δh(m)	v_S(m/s)
1	1.0	280	0.998	280.03
2	2.0	240	2.016	240.10
3	3.0	290	3.128	290.62
4	4.0	320	3.976	321.81
5	5.0	440	4.957	444.09
6	∞	620	∞	620.04

APPLICATION TO ACTUAL DATA

Our proposed method is further used to process a set of real surface wave data. The survey area is located in a mountain valley. In order to demonstrate the stratigraphic property, we laid out two crossed lines for survey. Data was recorded by using a 7 kg sledgehammer as impact source, and twelve 4.5 Hz geophones were lined up at the surface of the test sites (Fig. 9a). Offset is 2 m, receiver spacing is 2 m, shot spacing is 2 m, sampling is 0.2 ms, and sampling length is 2 K. Fig. 7 shows a shot original seismic record (the 10th shot) and its dispersion curve extraction.

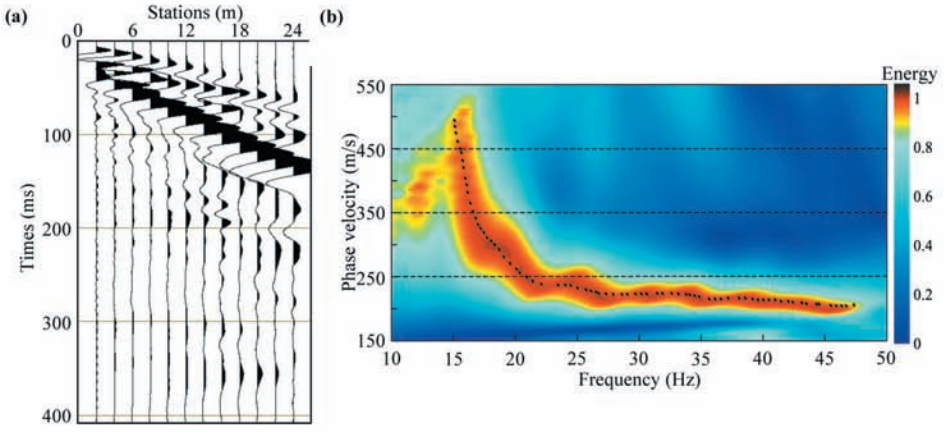

Fig. 7. Rayleigh wave dispersion curve extraction of the 10th shot data. (a) Original seismic data, (b) v_{Ph}-f spectrum and dispersion curve extraction.

Fig. 8a shows the inversion results by GA inversion and joint inversion. The GA is optimized by 20 iterations under the loose constraint of stratigraphic parameters, and the target is locked near the global optimal solution. Then the objective function residuals are rapidly converged from 1.86 by GA to 4.75E-4 by DLS after 84 iterations. The inversion results are almost completely coincident with the measured dispersion curves over the entire frequency distribution (Fig. 8b).

The 2D shear wave velocity profiles are obtained after inversion for each shot. The data interpretation is as follows:

1. The stratigraphy structure of the field can be divided into three layers. The first layer thickness is about 8 m, shear wave velocity v_S distribution between 150 and 450 m/s. It is attributed as artificial backfill. The second layer assumed as the weathering layer, the thickness is about 10 m, and the v_S is between 450 and 900 m/s. Stratigraphic ups and downs is more obvious, which mainly reflects the structural characteristics of the original strata. We presume the interface with 900 m/s as the bedrock interface because the v_S change gradient is larger at 16 m.

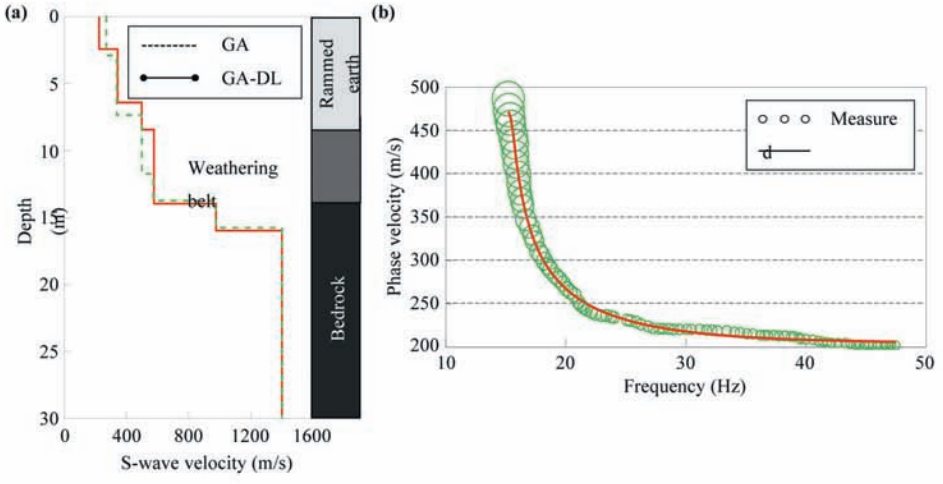

Fig. 8. Joint inversion results of the 10th shot data. (a) Stratigraphic structure (H-v_S), (b) Dispersion curve (v_{Ph}-f).

2. The intersection points A of both lines shows a good consistency of stratigraphic structure in the two v_S profiles. There is a depression between B (the 10th shot) and A is shown in Fig. 9b, which corresponds to the low-velocity abnormality tends to decrease from east to west between 15 and 40 m in Fig. 9c. Its formation is probably due to the long-term erosion by rain of east slope. A depression in the north of the field corresponds to the depression between 50 and 70 m in Fig. 9c.

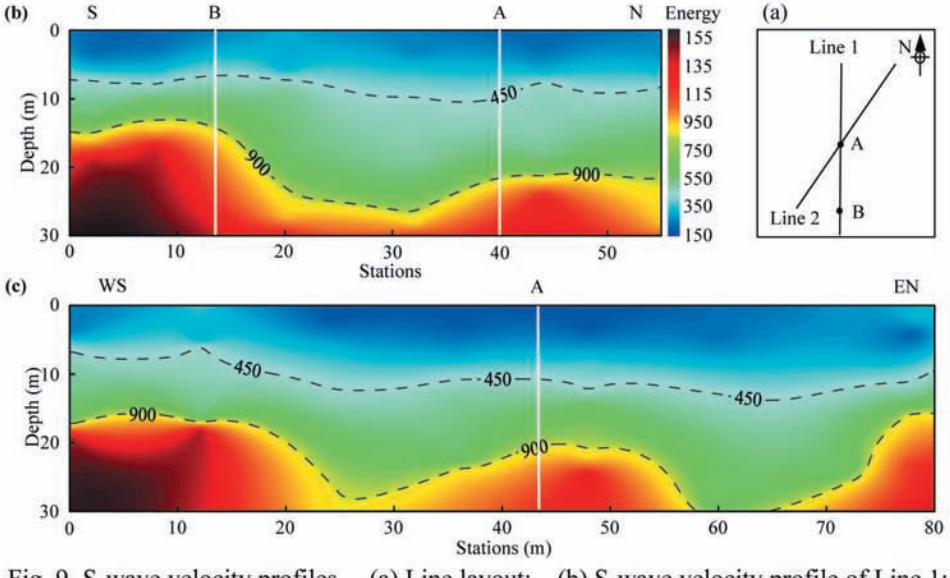

Fig. 9. S-wave velocity profiles. (a) Line layout; (b) S-wave velocity profile of Line 1; (c) S-wave velocity profile of Line 2.

CONCLUSIONS

Aiming at the Rayleigh wave dispersion curve inversion under complex geological conditions, we proposed a method of joint GA and DLS to inverse Rayleigh wave dispersion curve that combined with the advantages of linear inversion and non-linear inversion. We have made the following conclusions:

1. The conventional thin-layer DLS method reduces the initial model requirement to a certain extent. However, the multi-solution of the inversion results is exacerbate under complex seismic and geologic conditions attribution to the increase of the amount of inversion parameters. The applicability of GA inversion is stronger, but the extremely low efficiency cannot be ignored after dozens genetic optimizations. The drawbacks of the both methods can be complemented by each other, which produce the necessity to combine the GA and DLS inversion.

2. Under the constraints of the loose priori geological conditions, GA inversion can play the advantage based on global optimization retrieval. After dozens iterative operations, the target can be locked near the global optimal solution. Then a more accurate stratigraphic model can be got by DLS inversion to efficient local linear iterative optimization based on the rough model above. This is conducive to suppress the inversion multi-solution, reduce the dependence degree on the initial model, and improve the inversion quality.

ACKNOWLEDGEMENTS

This research was supported by the Shaanxi Province Natural Science Basic Research Project (No. 2017JZ007). Xi'an Shiyou University Graduate Innovation and Practical Ability Training Project (No. YCS17211027).

REFERENCES

Beaty, K.S., Schmitt, D.R. and Sacchi, M., 2002. Simulated annealing inversion of multimode Rayleigh wave dispersion curves for geological structure. Geophys. J. Internat., 151: 622- 631. doi: 10.1046/ j.1365-246X.2002.01809. x.

Caldwell, W.B., Klemperer, S.L., Rai, S.S. and Lawrence, J.F., 2009. Partial melt in the upper-middle crust of the northwest Himalaya revealed by Rayleigh wave dispersion. *Tectonophys*, 477: 58-65. doi: 10.1016/j.tecto. 2009.01.013.

Chang, J.P., de Ridder, S.A. and Biondi, B.L., 2016. High-frequency Rayleigh-wave tomography using traffic noise from long beach, California. Geophysics, 81: B43-B53. doi: 10.1190/GEO-2015 -0415.1.

Chen, X. and Sun, J., 2006. An improved equivalent homogenous half-space method and reverse fitting analysis of Rayleigh wave dispersion curve (in Chinese). Chin. J. Geophys., 49: 569-576. doi: 10.1002/ cjg2.859.

Cui, J., Liao, Z. and Huang, Z., 1994. Simplified stripping method for inversing shear wave velocity (in Chinese). China Civil Engin. J., 27: 50-58.

Guo, Z., Chen, Y. and Yin, W., 2015. Three-dimensional crustal model of Shanxi graben from 3D joint inversion of ambient noise surface wave and Bouguer gravity anomalies (in Chinese). Chin. J. Geophys., 58: 821-831. doi: 10.6038/cjg20150312.

Júnior, S.B.L., Prado, R.L. and Mendes, R.M., 2012. Application of multichannel analysis of surface waves method (MASW) in an area susceptible to landslide at Ubatuba City, Brazil. Revis. Brasil. Geofís., 30: 213-224.

Knopoff, L., 1964. A matrix method for elastic wave problems. Bull. Seismol. Soc. Am., 54: 431-438.

Laake, A., Strobbia, C. and Cutts, A., 2008. Integrated approach to 3D near surface characterization in desert region. First Break, 26: 109-112.

Liu, B., Liu, Z., Song, J., Nie, L., Wang, C. and Chen, L., 2017. Joint inversion method of 3D electrical resistivity detection base on inequality constraints (in Chinese). Chin. J. Geophys., 60: 820-832. doi:10.6038/cjg 20170232.

Luo, Y., Xia, J., Liu, J. and Liu, Q., 2008. Joint inversion of fundamental and higher mode Rayleigh waves (in Chinese). Chin. J. Geophys., 51: 242-249.

Lu, J., Li, S., Li, W. and Tang, L., 2014. A hybrid inversion method of damped least squares with simulated annealing used for Rayleigh wave dispersion curve inversion. Earthq. Engineer. Vibrat., 13: 13-21. doi:10.1007/s11803-014-0208-2.

Malagnini, L., Herrmann, R.B., Biella, G. and Franco R.D., 1995. Rayleigh waves in Quaternary alluvium from explosive sources: determination of shear-wave velocity and Q structure. Bull. Seismol. Soc. Am., 85: 900-922.

Madsen, K., Nielsen, H.B. and Tingleff, O., 2004. Methods for Non-Linear Least Squares Problems. Lecture Note.

Moro, G.D., Pipan, M., Forte, E. and Finetti, I., 2003. Determination of Rayleigh wave dispersion curves for near surface applications in unconsolidated sediments. Expanded Abstr., 73rd Ann. Internat. SEG Mtg., Dallas: 1247-1250. doi:10.1190/1.1817508.

Moro, G.D., Pipan, M. and Gabrielli, P., 2007a. Rayleigh wave dispersion curve inversion via genetic algorithms and Marginal Posterior Probability Density estimation. J. Appl. Geophys., 61: 39-55. doi:10.1016/j. jappgeo.2006.04.002.

Moro, G.D., Pipan, M. and Gabrielli, P., 2007b. Joint inversion of surface wave dispersion curves and reflection travel times via multi-objective evolutionary algorithms. J. Appl. Geophys., 61: 56-81. doi:10.1016/j.jappgeo.2006.04.001.

Nazarian, S., Stokoe, K.H. II and Hudson, W., 1983. Use of spectral analysis of surface waves method for determination of module and thicknesses of pavement systems. Transport. Res. Rec., 930: 38-45.

Park, C.B., Mille R.D. and Xia, J., 1999. Multichannel analysis of surface wave. Geophysics, 64: 800-808. doi:10.1190/ 1.1444590.

Meier, R.W. and Rix, G.J., 1993. An initial study of surface wave inversion using artificial neural networks. Geotech. Test. J., 16: 425-431. doi:10.1520/GTJ10282J.

Shen, H., Chen, C., Yan, Y. and Zhang, B., 2016. Multiple-transient surface wave phase velocity analysis in expanded f-k domain and its application. J. Seismic Explor., 25: 299-319.

Strobbia, C.L., Vermeer, P.L., Laake, A., Glushchenko, A. and Re, S., 2010a. Surface waves: processing, inversion and removal. First break, 28: 85-91.

Strobbia, C.L., Eman, A.E., Al-Genai, J. and Roth, J., 2010b. Rayleigh wave inversion for the near-surface characterization of shallow targets in a heavy oil field in Kuwait. First Break, 28: 103-109.

Strobbia, C.L., Laake, A., Vermeer, P. and Glushchenko, A, 2011. Surface waves: use them then lose them. Surface-wave analysis, inversion and attenuation in land reflection seismic surveying. Near-Surf. Geophys., 9: 503-513. doi: 10.3997/1873-0604.2011022.

Sussmann, T.R., Thompson, H.B., Stark, T.D., Wilk. S.T. and Ho, C.L., 2015. Use of seismic surface wave testing to assess track substructure condition. Railway Engineering Conf., Edinburgh.

Xia, J., Miller, R. and Park, C.B., 1999. Estimation of near-surface shear-wave velocity by inversion of Rayleigh wave. Geophysics, 64: 691-700. doi:10.1190/1.1444578.

Xia, J., Millller, R., Park, C., Hunter, J., Harris, J. and Ivanov, J., 2002a. Comparing shear wave velocity profiles inverted form multichannel surface wave with borehole measurements. Soil Dynam. Earthq. Engineer., 22: 181-190. doi:10.1016/S0267-7261(02)00008-8.

Xia, J., Millller, R., Park, C. and Tian, G., 2002b. Determining Q of near-surface materials form Rayleigh waves. J. Appl. Geophys., 51: 121-129. doi:10.1016/S0926-9851(02)00228-8.

Xia, J., Miller, R.D., Park, C.B. and Tian, G., 2003. Inversion of high frequency surface waves with fundamental and higher modes. J. Appl. Geophys., 52: 45-57. doi:10.1016/ S0926- 9851(02)00239-2.

Xia, J., Miller, R., Park, C.B., Ivanov, J., Tian, G. and Chen, C., 2004. Utilization of high-frequency Rayleigh waves in near-surface geophysics. The Leading Edge, 23 753-759. doi:10.1190/1. 1786895.

Xia, J., Xu, Y., Luo, Y., Miller, R., Cakir, R. and Zeng, C., 2012. Advantages of using multichannel analysis of Love waves (MALW) to estimate near surface shear-wave velocity. Surv. Geophys., 33: 841-860. doi: 10.1007/s10712-012-9174-2.

Xia, J., Gao, X., Pan, Y., Shen, C. and Yi, X., 2015. New findings in high-frequency surface wave method. Chin. J. Geophys., 58: 2591-2605. doi:10.6038/cig20150801.

Yamanaka, H. and Ishida, H., 1996. Application of genetic algorithms to an inversion of surface-wave dispersion data. Bull. Seismol. Soc. Am., 86: 436-444.

Yilmaz, Ö., Eser, M. and Berilgen, M., 2005. A case study of seismic zonation in municipal areas. The Leading Edge, 25: 319-330. doi: 10.1190/1.2147874